

Anatomical differences in the structural elements of fluid passage of Scots pine sapwood with contrasting treatability

Katrin Zimmer · Andreas Treu ·
Katherine A. McCulloh

Received: 13 May 2013 / Published online: 1 February 2014
© Springer-Verlag Berlin Heidelberg 2014

Abstract Treatability of wood is a function of anatomical properties developed under certain growing conditions. While Scots pine sapwood material normally is considered as easy to impregnate, great variations in treatability can be observed. In order to study anatomical differences in the structural elements of transverse fluid passage, wood material with contrasting treatability has been compared. Ray composition and resin canal network, membrane areas of fenestriform pits in the cross-field as well as dimension and properties of bordered pits were investigated. The results showed large anatomical differences between the two contrasting treatability groups. Refractory Scots pine sapwood samples developed more rays per mm² tangential section, while they were on average lower in cell numbers than rays found in easily treatable material. Easily treatable material had more parenchyma cells in rays than refractory material. At the same time, a larger membrane area in fenestriform pits in the cross-field was observed in the easily treatable sample fraction. Differences in the composition of resin canal network were not observed. Refractory samples developed on average smaller bordered pit features, with relatively small formed pit apertures compared to the easily treatable samples. In refractory Scots pine sapwood material, the structural elements of fluid passage such as bordered pit dimensions, fenestriform pits in the cross-field and parenchyma cells

K. Zimmer (✉) · A. Treu
Norwegian Forest and Landscape Institute, Pb 115, 1431 Ås, Norway
e-mail: katrin.zimmer@skogoglandskap.no

K. Zimmer
Department of Ecology and Natural Resource Management, Norwegian University of Life Sciences,
Pb 5003, 1432 Ås, Norway

K. A. McCulloh
Department of Forest Ecosystems and Society, Oregon State University, Corvallis, OR 97331, USA

K. A. McCulloh
Department of Botany, University of Wisconsin-Madison, Madison, WI 53706, USA

were altogether developed in smaller dimensions or number. Wood samples from better growing conditions and sufficient water supply showed a better treatability in this study.

Introduction

Impregnation of wood with protective agents depends on the treatability of the substrate. Wood anatomy as well as composition and properties of the impregnation agent influence the penetration of liquids in wood. Large differences in treatability exist between different softwood species. While Norway spruce is difficult to treat after drying (Flynn 1995), Scots pine sapwood can be impregnated easily (EN350-2 1994). However, considerable differences in treatability occur between different pine species (Bauch et al. 1983) and within Scots pine sapwood (Larnøy et al. 2008; Lande et al. 2010; Buro and Buro 1959b). The treatability of a typically permeable wood species can be influenced by geographic origin and the materials' growing conditions (Lande et al. 2010; Larnøy et al. 2008).

Scots pine has a large natural geographic distribution, covering boreal Eurasia, spreading southward to areas in Spain and Turkey (Mátyás et al. 2004). Therefore, the species needs to adapt to a large variation in environments and growing conditions, accompanied by hydraulic and anatomical adjustments (Antonova and Stasova 1993; Berninger 1997; Poyatos et al. 2007; Yaman 2007; Martínez-Vilalta et al. 2009; Lande et al. 2010; Martin et al. 2010).

In dried conifers, liquids take different pathways during impregnation. In longitudinal and tangential direction, liquids move through the tube system that is built up by axial tracheids, which are interconnected by bordered pits. Attributed to the major role in interconnecting the tracheid system in the stem, number, size and aspiration state of the bordered pits greatly influence the treatability of coniferous sapwood (Stamm 1947; Banks 1970), with aspirated bordered pits blocking fluid flow. Small diameter latewood tracheids as well as the portion of unaspirated pits in the latewood fraction positively influence treatability (Sedighi-Gilani et al. 2012; Phillips 1933). Radially, fluid transport occurs through the rays and is an important contributor to the overall treatability of the material (Côté 1963). In Scots pine, the rays consist of ray tracheids and ray parenchyma (Wagenführ 2007), the latter with thin, often unlignified cell walls (Wagenführ 1999). Between ray parenchyma and axial tracheids, half bordered pits are formed, so called fenestriform pits in Scots pine that indicate good communication between ray parenchyma and the axial tracheid system. However, the role of parenchyma rays is discussed controversially in the literature and might be dependent on the molecule size and liquid properties of the impregnation agent (Buro and Buro 1959a; Scholz et al. 2010). Fluid passage through the parenchyma was observed, and the possibility of membrane rupture or cell collapse indicated (Bamber 1973; Olsson et al. 2001a; Tondi et al. 2013). In a study comparing the treatability of different pine species, Bauch et al. (1983) found declining treatability with decreasing size of the half bordered pits in cross-fields. Species with large fenestriform pit areas and non-lignified ray parenchyma cells, such as Scots pine, were easiest to treat.

An investigation of structural differences between penetrated and non-penetrated material within Scots pine sapwood showed that the frequency of axial resin canals and the percentage of canals blocked, influenced the distribution of the preservative (Ahmed et al. 2012). Though it was also mentioned that the axial resin canal system did not participate in fluid transportation during impregnation (Tondi et al. 2013), the influence might be determined by the impregnation solution (Buro and Buro 1959a).

Detailed knowledge of anatomical differences between differently treatable Scots pine sapwood could optimize impregnation process times and positively influence production capacity and costs of manufacturing treated wood and impregnation of modified lumber. It is therefore important to know the main anatomical factors that influence treatability of Scots pine sapwood.

The main objective of this study is to analyze anatomical differences within Scots pine sapwood with contrasting treatability related to impregnation by wood protection agents. The specific objectives are (1) to analyze differences in ray composition and ray frequency, (2) to analyze the density of resin canal network, (3) to analyze fenestriform pore areas and (4) to study the bordered pit structure and dimensions.

Materials and methods

Material selection

For a study on anatomical differences of Scots pine sapwood with contrasting treatability, anatomical measurements were performed on eleven samples from seven different locations in Finland (F4), Norway (N1, N2, N3 and N4) and Scotland (Sc1 and Sc2) (Table 1). The material is a subset of a larger sample set, including sample material from 25 stands (225 trees in total) that all underwent the same impregnation schedule (5 min: 0.004 MPa and 10 min: 0.8 MPa) when impregnated with an experimental impregnation mix (aqueous furfuryl alcohol (FA) solution, 69 % water, 28 % FA and 3 % additives; Kebony AS, Skien, Norway). Impregnation was performed on pre-dried (48 h/40 °C) and conditioned (65 %RH/20 °C) samples (20 × 20 × 50 mm³) with sealed cross-sections to assure penetration only from the lateral surfaces. Weight and dimensions were recorded before and after impregnation. The applied process times are deliberately too short to achieve a full treatment. To analyze the penetration, the ratio of filling (RoF) (Lande et al. 2010) and the impregnated area (%) on the cross-section of the sample were calculated. The ratio of filling (RoF) gives a value of the actually filled volume of the sample related to the void volume, which theoretically could be filled. The ratio of filling in the entire sample pool varied from 84.7 % (F4-1) to 16.1 % (N3-1) with a grand mean of 43.3 % and a standard deviation of 15.4 %. Results on the variation of the ratio of filling of the whole dataset are reported in another article.

The eleven specimens within this study were untreated sibling samples, which were randomly taken from the 15 highest (RoF > 74 %) and lowest (RoF < 24 %) impregnated samples from the larger sample pool (Table 1). RoF was the only and

Table 1 Sample description, growing conditions and origin

Sample	Treatability			Climate		Location			Site index	
	group (RoF)	RoF	Imp. area	MAT	MAP	LAT	LONG	ALT	AHI	ARW
Sc1-1	High	74.6	100	9.01	627	57°39'N	3°39'W	20	0.249	1.25
Sc2-1	High	75.1	100	8.40	576	57°33'N	4°17'W	70	0.274	2.00
Sc2-2	High	77.4	100	9.17	652	57°33'N	4°17'W	70	0.317	2.22
Sc2-3	High	83.9	100	9.17	646	57°33'N	4°17'W	70	0.274	2.00
F4-1	High	84.7	100	6.44	623	60°01'N	23°02'E	55	0.349	1.11
N3-1	Low	16.1	37	2.31	534	62°37'N	9°48'E	575	0.109	0.36
N2-1	Low	16.6	49	2.59	550	62°37'N	9°48'E	575	0.111	0.77
N3-2	Low	17.5		2.29	528	62°37'N	9°48'E	575	0.117	0.42
N3-3	Low	18.5	47	2.42	538	62°37'N	9°48'E	575	0.120	0.53
N1-1	Low	20.6	74	2.28	660	66°52'N	15°17'E	70	0.147	0.80
N4-1	Low	20.7	48	2.20	590	61°40'N	11°16'E	431	0.102	0.57

RoF ratio of filling (%), *Imp. area* impregnated area (%), *MAT* mean annual temperature during growth (°C), *MAP* mean annual precipitation during growth (mm), *LAT* latitude, *LONG* longitude, *ALT* altitude, *AHI* annual height increment (m/a), *ARW* annual ring width (mm)

stand-independent selection criterion as the anatomical differences between these two contrasting groups of treatability were supposed to be studied. Untreated material which was located longitudinally directly adjacent to the impregnated material in the stem was used, and the respective sample material was considered alike due to the close proximity.

The refractory samples (16.1–20.7 % RoF) came from four different locations in Norway, all with low mean annual temperatures (MAT) during growth (2.20°–2.59 °C). Low MAT, high elevation of the stand and locations farther north are reflected in poor annual height increments (AHI = 0.102–0.147 m/a) and narrow annual ring width (ARW = 0.36–0.80 mm) in refractory samples. The easily treatable sample subset (74.6–84.7 % RoF) grew at locations farther south with higher annual temperatures during growth (6.44 °C in Finland, 8.4°–9.17 °C in Scotland), which is reflected in greater AHI (0.249–0.349 m/a) and wider ARW (1.11–2.22 mm) (Table 1).

The lateral treatability clearly differed between the two treatability groups. Samples with a high RoF were impregnated on 100 % of the cross-sectional area, whereas most of the samples from the low RoF group had less than 50 % of the cross-section impregnated. Because of this large difference, lateral penetration pathways were analyzed.

Preparation of slides for microscopy

Wood blocks for microscopic analysis with dimensions $20 \times 10 \times 10 \text{ mm}^3$ ($r \times t \times l$) were softened in purified water for 24 h before sectioning. Tangential and radial sections were prepared at a thickness of 14–20 μm using a Reichert sliding microtome. The sections were stained in 0.001 % safranin for 2 min,

dehydrated in a succession of 50, 75 and 96 % ethanol for 30 s each and finally mounted in Pertex on a microscope slide.

Anatomical measurements

Tangential images were recorded ($\times 5$) using a Leica DMR light microscope with a Leica DFC 425 camera and analyzed with the Leica application suite 3.7.0 software. Tangential sections were used in order to count and measure frequency and dimensions of rays and their structure composed of ray parenchyma and ray tracheids (Fig. 1c). Three areas of 1 mm^2 each were captured for the respective sample; the total number of rays and the composition of each ray were recorded.

Images from radial sections were acquired ($\times 20$) with a microscope-mounted digital camera (Micropublisher 5.0 RTU, QImaging, Surrey, B.C., Canada) and Q Capture Pro imaging software (QImaging Canada) on a Nikon Eclipse E400 compound microscope (Nikon Instruments, Melville, NY, USA). For image analysis, the image-analysis program ImageJ (National Institutes of Health, Bethesda, MD, USA; <http://rsb.info.nih.gov/ij/>) was used.

Radial images were used in order to measure the membrane area of fenestriform pits in the cross-field between ray parenchyma cells and axial tracheids of samples with contrasting treatability. Therefore, fifty membranes per sample were measured in earlywood areas excluding the first ring of tracheids in the season, as they often appeared narrower. The width of the cross-field associated tracheid was recorded as well as the total cross-field area. Secondly, dimensions of earlywood bordered pits of samples with different treatability and growing conditions were compared. In order to do so, the area of pit chambers, pit apertures and the diameter of the torus of fifty pits per sample were measured.

Statistical analysis

For the statistical data analysis, the JMP version 10.0 software (2012) from SAS Institute Inc. (Cary, North Carolina) was used. In order to compare the two treatability groups (refractory and easily treatable), sample averages were calculated ($n = 11$). Differences between groups were determined with ANOVA on a 0.1 (A) or 0.05 (B) significance level ($df = 9$).

Results

The average number of rays per mm^2 in tangential sections was significantly ($P = 0.0122$) higher in the refractory group compared to the easily treatable group of material. At the same time, these refractory samples had lower ray height ($P = 0.0323$) and higher total number of ray tracheids per mm^2 compared to easily treatable material. For the easily treatable samples, however, the total ray height and number of cells were higher with more parenchyma cells per ray and mm^2 . This relationship was reflected in the different parenchyma:tracheid ratios for the samples with contrasting treatability; high RoF samples had 0.89 parenchymatous

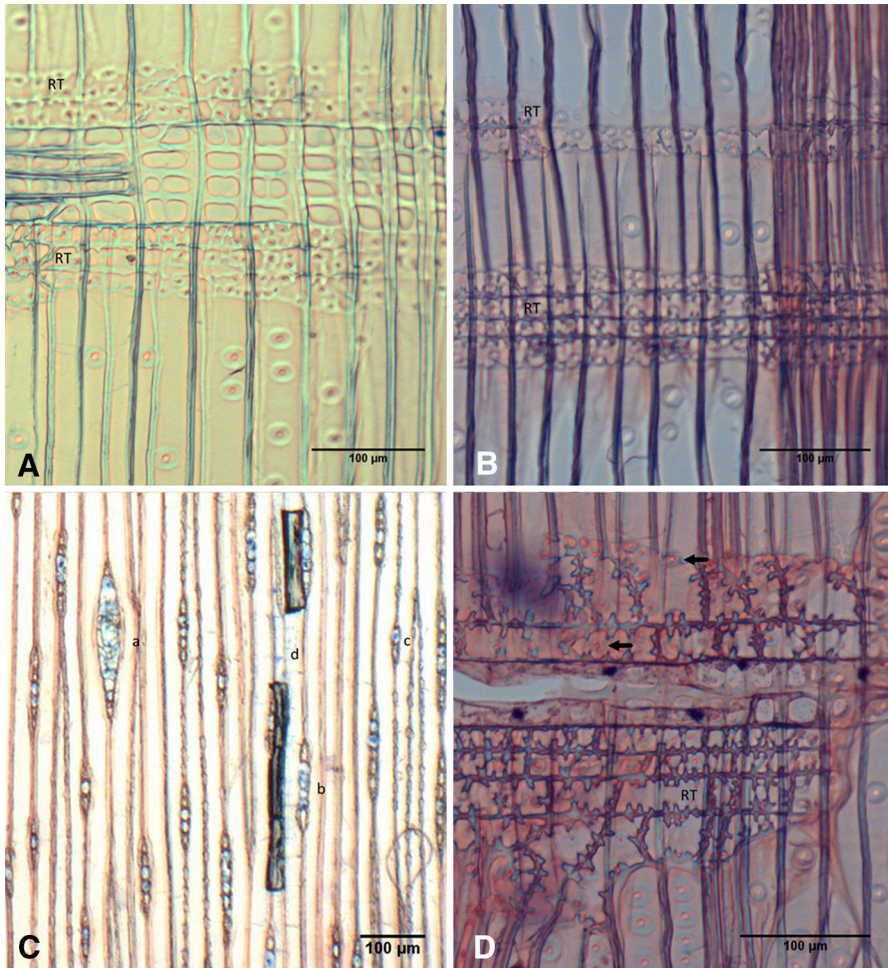


Fig. 1 **a** Ray in radial section, composed of two ray tracheids (RT) above and three rows of ray tracheids (RT) underneath a ray parenchyma (RP) area with four rows; on the cross-fields, window-like (fenestriform) half bordered pits can be seen; both one and two membranes per cross-field are present; **b** detail of two rays consisting entirely of ray tracheids (RT); **c** tangential section showing rays with different composition **a** fusiform ray with resin canal in center, **b** ray with five parenchyma cells, **c** ray with one parenchyma cell and one ray tracheid, **d** axial resin canal with thin-walled unligified parenchyma cells; **d** detail of ray tracheid pittings (*arrow*), the clearly dentate cell walls and large dimensions of the tracheids (RT) in a refractory sample with very narrow annual growth ring

cells per tracheid, whereas wood with low RoF only counted 0.62 ($P = 0.0769$, Table 2).

For the samples investigated, no significant differences in the composition of the resin canal network were observed (Table 2).

The tracheid diameters were similar in tissues with contrasting treatability, with an average diameter of 38 μm . However, the total cross-field and membrane areas were somewhat larger in easily treatable material compared to refractory material at

Table 2 Ray composition and resin canal network per 1 mm² tissue in easily treatable ($n = 5$) and refractory ($n = 6$) Scots pine sapwood samples

	Treatability group (RoF)	Average	Std dev	Min	Max	<i>P</i> value	<i>F</i> value
Rays/mm ²	High ($n = 5$)	28.77	3.21	22	35	0.0122 ^{a,b}	9.77
	Low ($n = 6$)	34.78	3.15	28	44		
Ray height (nr of cells)	High	5.86	0.66	1	13	0.0323 ^{a,b}	6.40
	Low	5.02	0.44	1	13		
Total ray height (μm)	High	135.64	15.19	11.90	410.70	0.0634 ^a	4.48
	Low	119.63	9.82	21.60	365.50		
No. of parenchymatous cells/ray	High	2.53	0.48	0	8	0.0065 ^{a,b}	12.37
	Low	1.84	0.11	0	6		
No. of tracheids/ray	High	3.33	0.68	0	10	0.6800	0.18
	Low	3.19	0.42	0	10		
Parenchyma:tracheid ratio	High	0.89	0.31	0	7	0.0769 ^a	3.99
	Low	0.62	0.10	0	3		
No. of parenchyma/mm ²	High	71.63	12.76	54	98	0.1558	2.40
	Low	62.72	5.68	48	83		
No. of ray tracheids/mm ²	High	93.32	15.00	62	127	0.0553 ^a	4.84
	Low	108.39	7.09	85	132		
No. of fusiform rays/mm ²	High	0.49	0.15	0.13	1.04	0.6501	0.22
	Low	0.54	0.13	0	1.04		
No. of axial resin canals/mm ²	High	0.51	0.17	0.36	0.70	0.7602	0.10
	Low	0.54	0.12	0.43	0.73		

Different letters indicate statistically significant differences between treatability groups at ^a $P < 0.1$ and ^b $P < 0.05$

a $P < 0.1$ (Table 3). The combination of large membrane areas with generally higher numbers of ray parenchyma cells in easily treatable material leads to a significantly larger total membrane area in easily treatable material.

The bordered pit dimensions showed significant differences between the groups with contrasting treatability in all tested properties (Table 4). The diameters of the aperture ($P = 0.0087$), torus ($P = 0.0194$) and pit chamber ($P = 0.0819$) all had larger average dimensions for the easily treatable material. In total, the minimum and maximum measured dimensions for the pits showed for all results large ranges within the respective treatability groups. Both ratios, torus:aperture and pit chamber : aperture, were significantly different between the treatability groups ($P = 0.0459$; 0.01 , respectively). The values showed that the aperture diameters of refractory samples are small as compared with easily treatable samples.

Discussion

This study shows the influence of anatomical differences within Scots pine sapwood material with contrasting treatability in relation to the treatability with wood

Table 3 Fenestriform pits in the cross-field in Scots pine: dimensions of the total cross-field area and the respective area of fenestriform pits in the cross-field

	Treatability group (RoF)	Average	Std dev	Min	Max	<i>P</i> value	<i>F</i> value
Tracheid width (μm)	High	39.80	4.66	24.08	66.00	0.3690	0.89
	Low	37.77	2.27	24.05	58.53		
Total area cross-field (μm^2)	High	875.58	94.48	452.50	1672.25	0.0989 ^a	3.39
	Low	790.08	58.80	278.00	1,341.75		
Total membrane area (μm^2)	High	384.09	31.66	114.00	793.80	0.0725 ^a	4.14
	Low	346.78	29.16	24.00	692.50		

Different letters indicate statistically significant differences between treatability groups at ^a $P < 0.1$ and ^b $P < 0.05$

Table 4 Dimensions and proportions of bordered pit properties in earlywood with contrasting treatability

	Treatability group (RoF)	Average	Std dev	Min	Max	<i>P</i> value	<i>F</i> value
Aperture diameter (μm)	High	3.94	0.33	2.80	5.21	0.0087 ^{a,b}	11.14
	Low	3.36	0.24	2.23	4.42		
Torus diameter (μm)	High	9.82	0.32	8.27	12.23	0.0194 ^{a,b}	8.07
	Low	9.16	0.40	6.95	11.10		
Pit chamber diameter (μm)	High	20.55	0.71	15.87	23.66	0.0819 ^a	3.84
	Low	19.72	0.69	16.01	23.35		
Torus:aperture ratio	High	2.52	0.14	1.77	3.35	0.0459 ^{a,b}	5.35
	Low	2.77	0.21	1.93	3.75		
Pit chamber:aperture ratio	High	5.27	0.35	4.08	7.12	0.0100 ^{a,b}	10.57
	Low	5.95	0.34	4.38	8.34		

Different letters indicate statistically significant differences between treatability groups at ^a $P < 0.1$ and ^b $P < 0.05$

protection agents. The ray composition and frequency showed, in general, significant differences between the groups with high and low treatability wood material. The parenchyma associated with the rays seems to have a strong influence on treatability, and characteristically wood which is easily treatable has a significantly higher number of parenchyma per ray than refractory wood. The importance of ray parenchyma on treatability is supported by the ray parenchyma:ray tracheid ratio, which is significantly higher for easily treatable material with 0.89 (± 0.31) in contrast to the ratio of refractory material with 0.62 (± 0.10). A relatively low ratio of 0.66 is reported for rays from Northern German Scots pine material (ARW = 6.6 mm) (Bauch et al. 1983) that was tested as easiest to treat in comparison with different pine species.

Refractory material, however, has a higher number of ray tracheids ($P = 0.0553$) and at the same time a higher total number of rays per mm^2 (high 28.77 ± 3.21 , low

34.78 ± 3.15 ; $P = 0.0122$) with a lower ray height compared to easily treatable material. The ray height (number of cells) measured in the current study (high RoF 5.86 ± 0.66 , low RoF 5.02 ± 0.44 ; A) is in general lower compared to values given in literature with an average of nine cells in height (Wagenführ 2007). In other studies, average ray heights of 7.3–7.5 cells are reported (Yaman 2007; Ahmed et al. 2012). The same tendency can be seen for the measured values of ray height in length (high RoF: $135.64 \mu\text{m} \pm 15.19$, low RoF: $119.63 \mu\text{m} \pm 9.82$; A), whereas Yaman (2007) measured ray heights of $190 \mu\text{m} (\pm 58.2)$, which were again greater in Turkish Scots pine. In general, ray heights of 70–500 μm are reported (Wagenführ 2007), which presumably included both small uniseriate rays and fusiform rays.

Rays are composed of parenchyma cells and tracheids (Fig. 1a, c, d). They are predicted to have an important dual role in the radial water and nutrient supply on the one hand and storage of carbohydrates and secondary derivatives on the other hand (Pallardy 2008). With small growth rings, as found in the refractory material in this study (Table 1), more annual rings are necessary in the living tree to maintain sufficient sap flow (Gartner and Meinzer 2005). Radial tracheids provide sufficient water supply between longitudinal tracheids (Brown 1915; Wagenführ 1999). In refractory wood that grew under dry and cold conditions (Table 1), the need to avoid embolism proliferation is present. Hence, precautions in the water supply and conductive system are important and engender alterations in pit dimensions and the composition of the radial water supply. More radial connections between the longitudinal tracheids are formed in the form of a higher number of tracheid-composed radial connections (Fig. 1b, c). This connectivity could ensure radial water transport even in the case of failure of some parts of the sapwood as more connections to more longitudinal tracheids are built. To withstand high turgidities, the cell walls of the radial tracheids show spiral reinforcements that appear as dendroid structures in radial microscopy sections (Wagenführ 1989). Figure 1d demonstrates areas of massively reinforced cell walls in ray tracheids in a refractory sample. In fluid flow experiments with dye tracers in *Ponderosa* pine and Douglas-fir wood, however, no infiltrations into the ray tracheids were observed (Barnard et al. 2013). In the wood of *Cryptomeria japonica*, other transverse pathways such as a radial grain of earlywood tracheids, intercellular spaces alongside the rays and tangential wall pittings in the earlywood and latewood close to the growth ring boundary were identified (Kitin et al. 2009). Bamber (1973) reports on interstitial spaces that form during drying caused by collapse of the thin-walled unlignified cell walls of epithelia cells of the resin canal system and parenchyma cells of the rays. The parenchyma cell walls are reported to be mostly unlignified in Scots pine, though lignified cell walls are also present (Bauch et al. 1983), and lignification is a process in cell maturation that can occur prior to heartwood formation (Balatinecz and Kennedy 1967). The differences in treatability could as a consequence also be a result of different proportions of lignified parenchyma cell walls due to aging processes of samples with different annual ring widths.

The total membrane area of fenestriform pits in the cross-field between ray parenchyma and axial tracheids was significantly larger ($P = 0.0725$) for easily treatable wood material ($384.09 \mu\text{m}^2 \pm 31.66$) compared to refractory material

($346.78 \mu\text{m}^2 \pm 29.16$). These values are lower compared to the average of $460 \mu\text{m}^2$ measured in Scots pine from Northern Germany (Bauch et al. 1983).

The combination of total membrane area in the cross-fields and the higher number of ray parenchyma in easily treatable wood material lead to a higher proportion of conductive areas, which can be used as impregnation pathways. It was found that an increasing area of fenestriform pits in the cross-field and unligified ray parenchyma cell walls led to higher uptake of impregnation agents when comparing the treatability of different pine species (Bauch et al. 1983). The ray parenchyma complex is often associated with fluid transportation and allocation to adjacent tracheids, though this function is often attributed to the rupture and collapse of the thin unligified cell walls and fenestriform pits in the cross-field (Wardrop and Davies 1961; Bamber 1973; Olsson et al. 2001a, b; Tondi et al. 2013).

The proportions of earlywood bordered pits of material with contrasting treatability in this study were significantly different. All features of the bordered pit such as pit aperture diameter (high RoF: $3.94 \mu\text{m} \pm 0.33$; low RoF $3.36 \mu\text{m} \pm 0.24$; $P = 0.0087$), torus diameter (high RoF $9.82 \mu\text{m} \pm 0.32$; low RoF $9.16 \mu\text{m} \pm 0.40$; $P = 0.0194$) and pit chamber diameters (high RoF $20.55 \mu\text{m} \pm 0.71$; low RoF $19.72 \mu\text{m} \pm 0.69$; $P = 0.0819$) were significantly greater for easily treatable material. The measured values of torus diameters and pit chamber diameters correspond to measurement results from literature, where torus diameters of $9.5 \mu\text{m}$ with a range of $8\text{--}12 \mu\text{m}$ and pit chamber diameters of $20 \mu\text{m}$ ($15\text{--}22$) were measured by Liese and Fahrenbrock (1952). Yaman (2007) found pit chamber diameters of $23.5 \mu\text{m}$ (± 1.5). Pit chamber dimensions within different proveniences and growing conditions in Spain varied from averages of $22.3 \mu\text{m}$ (± 2.1) to $27.9 \mu\text{m}$ (± 1.8) (Martin et al. 2010), where both sites were located in oroboreal climates, and significant differences between pit dimensions were found between different regions of the provenance. A total variation in pit chamber diameters of $15.3\text{--}32.7 \mu\text{m}$ was found in the Spanish study. Interestingly, the current results for the aperture diameter are smaller than the ones reported in literature of $5 \mu\text{m}$ ($4\text{--}6$) (Liese and Fahrenbrock 1952) and $5.9 \mu\text{m}$ (± 0.5) (Yaman 2007).

The average of the easily treatable material, though, is at the border of the variation given by Liese and Fahrenbrock (1952). One has to take into account the different water regimes and growing conditions at the respective sites, with the refractory material growing at lower MAT and relatively low MAP (Table 1) compared to German, Turkish, Scottish and Spanish Scots pine, as vulnerability to water-stress-induced embolism was found to be correlated with differences in the dimensions of torus and margo in Douglas-fir (Domec et al. 2006). Also, the torus diameter:pit aperture ratios were found to increase with height leading to a greater hydraulic resistance (Domec et al. 2008). An increased hydraulic resistance is reported to be correlated with smaller pit apertures (Domec et al. 2006). This fact could account for the small measured pit dimensions in refractory wood samples.

The results of the analyses of the bordered pits do not indicate whether and to what extent the bordered pits were involved in the transmission of impregnation agents during the treatment. In its dried condition, most of the bordered pits in the earlywood fraction of a growth ring are aspirated (Phillips 1933). However, whether

fluid passage occurred through an unspirated bordered pit fraction in earlywood or through collapsed pits with a stretched margo is unknown.

No differences were found between the resin canal systems of the material with contrasting treatability. Neither the axial resin canals nor the frequency of fusiform rays showed significant differences. Tondi et al. (2013) found the resin canals empty after treatment with tannin solutions, although Ahmed et al. (2012) found significant differences in the dimensions of both axial and radial resin canals between impregnated and unimpregnated areas within their study. Also, the number of axial resin canals/mm² was significantly higher in the impregnated material fraction. They found a consistency between impregnated areas and a minor blockage of the resin canals in this material compared to unimpregnated areas.

Conclusion

The study shows significant anatomical differences in Scots pine sapwood with contrasting treatability. Refractory material has a higher number of rays per mm². However, the samples display a lower ray height and a higher number of tracheids. Easily treatable Scots pine sapwood, in contrast, has a higher number of ray parenchyma cells leading to a generally increased area of fenestriform pits in the cross-field between ray parenchyma and longitudinal tracheids. These enlarged interconnections could greatly enhance transverse fluid passage within easily treatable material. The frequency of both radial and axial resin canals is not significantly different. Refractory samples developed on average smaller bordered pit features, with relatively small formed pit apertures compared to the easily treatable samples. In refractory Scots pine sapwood material, the structural elements of fluid passage such as bordered pit dimensions, fenestriform pits in the cross-field and parenchyma cells were altogether developed in smaller dimensions or in smaller number. Within the samples investigated in this study, a better treatability is found in samples growing under better growing conditions and sufficient water supply.

Acknowledgments The authors would like to thank the Northern Periphery Programme project “Developing the Scots pine Resource” for financial support within the sampling process. KAM’s participation in this project was funded by Grant IBN 09–19871 from the National Science Foundation, USA.

References

- Ahmed SA, Sehlstedt-Persson M, Karlsson O, Morén T (2012) Uneven distribution of preservative in kiln-dried sapwood lumber of Scots pine: impact of wood structure and resin allocation. *Holzforschung* 66(2):251–258
- Antonova GF, Stasova VV (1993) Effects of environmental factors on wood formation in Scots Pine stems. *Trees Struct Funct* 7(4):214–219
- Balatinecz JJ, Kennedy RV (1967) Maturation of ray parenchyma cells in Pine. *Forest Prod J* 17(10):57–64
- Bamber RK (1973) The formation and permeability of interstitial spaces in the sapwood of some pinus species. *J Inst Wood Sci* 6(2):36–38

- Banks WB (1970) Some factors affecting the permeability of Scots Pine and Norway Spruce. *J Inst Wood Sci* 5(25):10–17
- Barnard DM, Lachenbruch B, McCulloh KA, Kitin P, Meinzer FC (2013) Do ray cells provide a pathway for radial water movement in the stems of conifer trees? *Am J Bot* 100:322–331
- Bauch J, Liese W, Willeitner H (1983) Zum Tränkverhalten verschiedener Kiefernarten. *Holz Roh Werkst* 41(8):339–344
- Berninger F (1997) Effects of drought and phenology on GPP in *Pinus sylvestris*: a simulation study along a geographical gradient. *Funct Ecol* 11(1):33–42
- Brown FBH (1915) Variation in the size of ray pits in conifers. *Ohio Nat* 15(8):542–550
- Buro A, Buro E-A (1959a) Beitrag zur Kenntnis der Eindringwege für Flüssigkeiten in Kiefernholz. *Holzforschung* 3:71–77
- Buro A, Buro E-A (1959b) Untersuchungen über die Durchlässigkeit von Kiefernholz. *Holz Roh Werkst* 17(12):461–474
- Côté WA (1963) Structural factors affecting the permeability of wood. *J Poly Sci Part C Poly Symp* 2(1):231–242
- Domec JC, Lachenbruch B, Meinzer FC (2006) Bordered pit structure and function determine spatial patterns of air-seeding thresholds in xylem of Douglas fir (*Pseudotsuga menziesii*; Pinaceae) trees. *Am J Bot* 93:1588–1600
- Domec JC, Lachenbruch B, Meinzer FC, Woodruff DR, Warren JM, McCulloh KA (2008) Maximum height in a conifer is associated with conflicting requirements for xylem design. *PNAS* 105(33):12069–12074
- EN350-2 (1994) Durability of wood and wood-based products. Natural durability of solid wood. Guide to natural durability and treatability of selected wood species of importance in Europe. European Norm
- Flynn KA (1995) A review of the permeability, fluid-flow, and anatomy of Spruce (*Picea* spp.). *Wood Fiber Sci* 27(3):278–284
- Gartner BL, Meinzer FC (2005) Structure–function relationships in sapwood water transport and storage. In: Zwieniecki M, Holbrook NM (eds) *Vascular transport in plants*. Elsevier Academic Press, Oxford, pp 307–332
- Kitin P, Fujii T, Abe H, Takata K (2009) Anatomical features that facilitate radial flow across growth rings and from xylem to cambium in *Cryptomeria japonica*. *Ann Bot* 103(7):1145–1157
- Lande S, Høibø O, Larnøy E (2010) Variation in treatability of Scots pine (*Pinus sylvestris*) by the chemical modification agent furfuryl alcohol dissolved in water. *Wood Sci Technol* 44(1):105–118
- Larnøy E, Lande S, Vestøl GI (2008) Variations of Furfuryl alcohol and Wolmanit CX-8 treatability of pine sapwood within and between trees. Paper presented at the International Research Group on Wood Protection, Istanbul, Turkey, 25–29 May 2008
- Liese W, Fahrenbrock M (1952) Elektronenmikroskopische Untersuchungen über den Bau der Hoftüpfel. *Holz Roh Werkst* 10(5):197–201
- Martin JA, Esteban LG, de Palacios P, Fernandez FG (2010) Variation in wood anatomical traits of *Pinus sylvestris* L. between Spanish regions of provenance. *Trees Struct Funct* 24(6):1017–1028
- Martínez-Vilalta J, Cochard H, Mencuccini M, Sterck F, Herrero A, Korhonen JFJ, Llorens P, Nikinmaa E, Nolè A, Poyatos R, Ripullone F, Sass-Klaassen U, Zweifel R (2009) Hydraulic adjustment of Scots pine across Europe. *New Phytol* 184(2):353–364
- Mátyás C, Ackzell L, Samuel CJA (2004) EUFORGEN technical guidelines for genetic conservation and use for Scots pine (*Pinus sylvestris*). *Int Plant Genet Resour Inst*, Rome
- Olsson T, Megnis M, Varna J, Lindberg H (2001a) Measurement of the uptake of linseed oil in pine by the use of an X-ray microdensitometry technique. *J Wood Sci* 47(4):275–281
- Olsson T, Megnis M, Varna J, Lindberg H (2001b) Study of the transverse liquid flow paths in pine and spruce using scanning electron microscopy. *J Wood Sci* 47(4):282–288
- Pallardy SG (2008) *Physiology of woody plants*, 3rd edn. Elsevier Inc., Amsterdam
- Phillips EWJ (1933) Movement of the pit membrane in coniferous woods, with special reference to preservative treatment. *Forestry* 7(2):109–120
- Poyatos R, Martínez-Vilalta J, Cermak J, Ceulemans R, Granier A, Irvine J, Kostner B, Lagergren F, Meiresonne L, Nadezhdina N, Zimmermann R, Llorens P, Mencuccini M (2007) Plasticity in hydraulic architecture of Scots pine across Eurasia. *Oecologia* 153(2):245–259
- Scholz G, Krause A, Militz H (2010) Exploratory study on the impregnation of Scots pine sapwood (*Pinus sylvestris* L.) and European beech (*Fagus sylvatica* L.) with different hot melting waxes. *Wood Sci Technol* 44(3):379–388

- Sedighi-Gilani M, Griffa M, Mannes D, Lehmann E, Carmeliet J, Derome D (2012) Visualization and quantification of liquid water transport in softwood by means of neutron radiography. *Int J Heat Mass Transf* 55(21–22):6211–6221
- Stamm AJ (1947) Passage of liquids, vapors and dissolved materials through softwoods. Technical bulletin, US Forest Products Laboratory 929
- Tondi G, Thevenon MF, Mies B, Standfest G, Petutschnigg A, Wieland S (2013) Impregnation of Scots pine and beech with tannin solutions: effect of viscosity and wood anatomy in wood infiltration. *Wood Sci Technol* 47(3):1–12
- Wagenführ R (1989) Anatomie des Holzes, unter besonderer Berücksichtigung der Holztechnik. Fachbuchverlag, Leipzig
- Wagenführ R (1999) Anatomie des Holzes: Strukturanalytik, Identifizierung, Nomenklatur. Mikrotechnologie, DRW-Verlag, Leinfelden-Echterdingen
- Wagenführ R (2007) Holzatlas, 6th edn. Fachbuchverlag Leipzig, Carl Hanser Verlag
- Wardrop AB, Davies GW (1961) Morphological factors relating to the penetration of liquids into wood. *Holzforschung* 15(5):129–141
- Yaman B (2007) Comparative wood anatomy of *Pinus sylvestris* and its var. *compacta* in the west Black Sea region of Turkey. *IAWA J* 28(1):75–81